



Oxygen Reduction Reaction on Metal and Nitrogen–Doped Carbon Electrocatalysts in the Presence of Sodium Borohydride

Ricardo Sgarbi^{1,2} · Edson A. Ticianelli² · Frédéric Maillard¹ · Frédéric Jaouen³ · Marian Chatenet¹

Published online: 16 May 2020

© Springer Science+Business Media, LLC, part of Springer Nature 2020

Abstract

Metal and nitrogen–doped carbon electrocatalysts (M–N–C, where *M* is Fe or Co) were investigated for the oxygen reduction reaction (ORR) in alkaline conditions in the presence of borohydride ions (BH₄[−]). The electrochemical properties of the Fe–N–C and Co–N–C catalysts were investigated by cyclic voltammetry and rotating disk electrode techniques: their ORR electrocatalytic activity was bridged to their physicochemical properties, mainly type of metallic center (Fe vs. Co), structure (atomic dispersion vs. nanoparticles), and BET surface area. It is found that Fe–N–C catalysts have the best performances for the ORR electrocatalysis, even in the presence of BH₄[−] anions. The atomically dispersed Fe- and Co-containing electrocatalysts reach better BH₄[−]-tolerance than their counterparts bearing nanoparticles. For the atomically dispersed Fe–N–C electrocatalysts, the lowest BET surface area material generates a slight advantage of ORR mass activity and a poor (and desired) activity for borohydride oxidation reaction (BOR).

Keywords Metal-nitrogen–doped carbons (M–N–C) · Catalyst · Fe–N–C · Co–N–C · Oxygen reduction reaction · Direct borohydride fuel cells

Introduction

Small mobile electric devices (e.g., either portable electronics or drones) require power systems of high energy density. They are usually powered by batteries, but these “closed systems” are inherently limited by their insufficient specific energy (e.g., < 250 Wh kg^{−1} for the most energetic Li-ion systems [1]). Fuel cells, being open systems, are intrinsically denser in energy and could therefore advantageously be used in such devices. The present standard is the proton exchange membrane fuel cell (PEMFC), which is, in its state-of-the-art, fed

by pure hydrogen [2]. While transporting, compressing, and storing gaseous hydrogen may prove relevant for large quantities of energy stored, this solution is not always efficient, safe, economically viable, and therefore relevant in applications where smaller amount of energy is stored, i.e., the particular case for small mobile electric devices. In that situation, the direct oxidation of a liquid fuel may be more desirable, and direct methanol fuel cells (DMFC) have historically been studied as the pioneer direct liquid fuel cell (DLFC) [3]. However, electrooxidizing methanol is a complex and slow process (not speaking from the toxicity of the fuel), which requires extensive amounts of platinum-group-metal (PGM) electrocatalyst, and this is a clear hindrance to the development of DMFCs, should they be acidic or alkaline [2, 4]. While other hydrocarbon fuels have been tried as well, none proved capable to provide both sufficient energy and power density (even in alkaline environments, known to facilitate the reactions and hence to render them faster [5]), a clear drawback for the powering of small electronic devices. This triggered intense research to find more suitable liquid fuels for portable/small mobility application; from these works, sodium borohydride soon appeared as a promising candidate, owing to the properties of its fuel [6, 7] and of its relevance for portable fuel cell system design [8–11].

✉ Frédéric Maillard
Frederic.Maillard@lepmi.grenoble-inp.fr

✉ Marian Chatenet
Marian.Chatenet@grenoble-inp.fr

¹ CNRS, Grenoble INP (Institute of Engineering University of Grenoble Alpes), University of Grenoble Alpes LEPMI, 38000 Grenoble, France

² Instituto de Química de São Carlos, Universidade de São Paulo, Avenida Trabalhador São-carlense 400 Parque Arnold Schmidt, CP 780, São Carlos, SP 13560-970, Brazil

³ ICGM, Univ. Montpellier, CNRS, ENSCM, Montpellier, France

Of course, the direct oxidation of the borohydride anion (BH_4^-) in a direct borohydride fuel cell (DBFC) is not an easy process, and many works addressed the issue, so as to isolate the reaction mechanisms [12–18]; the proper electrocatalysts for the anode [19]; and the ideal fuel composition, electrode structure, operating parameters of the anode, etc. [20–23]. While one shall not neglect research actions to improve our understanding of the borohydride oxidation reaction (BOR) and hence to find better materials to achieve it efficiently, one must also not neglect the membrane/separator that should separate the anode and cathode compartments. To date, cation-exchange membranes are more mature than their anion-exchange counterparts, and bipolar membranes are at an early stage of development. All types of ion-exchange membranes can be used in a DBFC (see for example [24, 25]), and, whatever the nature of the membrane/separator, there are drawbacks to their utilization. For a cation-exchange membrane, during DBFC operation, the Na^+ cation shall migrate to the cathode, where it will combine with the OH^- species formed in the alkaline oxygen reduction reaction (ORR), thereby displacing the NaOH from the anolyte to the cathode side. This naturally has a clear detrimental effect on the operation of the cathode, as recently put forth by Ould-Amara et al. [26], owing to deleterious crystallization of NaOH in the cathode pores, leading to unavoidable mass-transport hindrances. Should an anion-exchange membrane be used (this is probably the desired situation, as the anolyte of a DBFC is necessarily alkaline [27, 28]), there will be non-negligible crossover of borohydride anions from the fuel anolyte to the cathode compartment. In that latter case, of course, the cathode catalyst must be tolerant to BH_4^- , otherwise its apparent ORR activity will be significantly affected, because either the net current will be the sum of the cathodic (desired) ORR and anodic (undesired) BOR contributions, or because borohydride species will adversely adsorb or react with the catalyst material and deactivate or chemically modify it. This shows that the cathode of a DBFC should also be tightly optimized, and in particular that BH_4^- -tolerant ORR catalysts must be selected for the application [10].

The literature regarding fuel-tolerant electrocatalysts for alkaline fuel cells is abundant, but mainly deals with tolerance to hydrocarbon molecules (methanol, ethanol, etc.) [29–33]. The case of borohydride, a very strong reducer, has been less under focus, even if some (rare) studies have explored the issue. Metal-oxides (e.g., perovskites, $\text{LaNi}_{0.8}\text{Co}_{0.2}\text{O}_3$ [34] and carbon-supported nanometric manganese oxides, MnO_x/C) [35, 36] have demonstrated some interesting properties for potential use in DBFC cathodes, but one could question the durability of such inherently oxidized materials in strongly reducing environments; as a matter of fact, long-term stability data was never reported in such studies, except for MnO_x/C (but not in the presence of BH_4^- species) [37]. Cheng and Scott [38] explored PGM-free electrocatalysts (iron

tetramethoxyphenyl porphyrin (FeTMPP), silver, and nickel), regarding their ORR performances in direct borohydride fuel cell cathodes. FeTMPP cathodes outperformed silver and nickel ones, which led the authors to the conclusion that FeTMPP was somewhat BH_4^- -tolerant, unlike Ag and Ni (the latter is no surprise, as both Ag [39, 40] and especially Ni [41–43] are active catalysts for the BOR). More recently Fe-aminoantipyrine (Fe-AAPyr) was successfully developed as a BH_4^- -tolerant ORR catalyst for a mixed-reactant DBFC [44]. These last two materials fall into the category of metal–nitrogen–carbon (M–N–C) catalysts, which are now under tremendous focus to replace Pt-based ones for PEMFC applications (see, e.g., [45–47]). Because these classes of material are commonly admitted to be tolerant to fuel species, and some of them have indeed shown tolerance to borohydride [38, 44], the present contribution explores two families of M–N–C compounds, based on cobalt (Co) and iron (Fe) metal centers. It notably aims to unveil whether any such catalysts are tolerant to BH_4^- , or if they must have particular features to be tolerant, herein are compared the nature of the metal (Fe and Co), the structure of the resulting electrocatalyst (atomically dispersed vs. nanoparticles), and its mode of synthesis (flash vs. ramp pyrolysis in argon atmosphere).

Materials and Methods

Catalyst Syntheses

The electrocatalysts used in this study were synthesized using the method described by Ranjbar-Sahraie et al. [48]. In brief, a zinc (II) zeolitic imidazolate framework (ZIF-8, purchased from BASF, Basolite Z1200), Fe or Co acetate precursor, and 1,10-phenanthroline were mixed via dry planetary ball milling. The masses of the precursors were 200 mg phenanthroline, 800 mg ZIF-8, and either 0.5 wt% or 5.0 wt% of metal (Fe or Co) compared with the overall mass of the three precursors. The dry mixed metal, carbon, and nitrogen precursors were then pyrolyzed either in flash (i.e., the powder was introduced at 1050 °C in the oven) or ramp (the powder was heated from room temperature to 1050 °C at 5 °C min^{-1}) mode, and a temperature of 1050 °C was maintained for 1 h. Then, the quartz tube and boat were opened and quenched to room temperature while still flowing Ar. As Ar was used, the weight loss during the pyrolysis was ca. 65–75 wt% and it was independent on the pyrolysis mode.

Physicochemical Characterizations

All physicochemical characterizations have been previously published; then, here only a brief overview is presented (for detailed experimental specifications, the readers could refer to References [48–52]). TEM measurements were performed on

a JEM-2100HCKM (JEOL) microscope operating at 120 keV for the atomically dispersed metal atom electrocatalysts [48, 50] and a JEOL 2010 TEM microscope operating at 200 kV for the metal nanoparticulated electrocatalysts [51]. To obtain ^{57}Fe Mössbauer spectra and confirm the absence of zerovalent iron crystalline phases in atomically-dispersed metal atom electrocatalysts, Fe-containing samples were measured with ^{57}Co –Rh source and analyzed for doublet and sextet spectral components ([51] for $\text{Fe}_{5.0}\text{RP}$ and $\text{Fe}_{0.5}\text{RP}$; [52] for $\text{Fe}_{0.5}\text{FP}$). The carbon nanocrystallites were characterized by Raman Spectroscopy using an argon LASER (514 nm) and X-ray diffraction by an X'Pert PRO MPD PANalytical diffractometer operated at 45 kV [51]. Surface area and pore volume were estimated by the Brunauer–Emmett–Teller (BET) method using a Micromeritics ASAP 2020 equipment with N_2 sorption at liquid nitrogen temperature (77 K) [49].

Electrochemical Characterizations

Before the electrochemical measurements, the glassware, polytetrafluoroethylene (PTFE)-based materials, volumetric flasks, tips, and electrodes were cleaned in 50% *v/v* solution of H_2SO_4 (Merck, Suprapur 96 wt%)/ H_2O_2 (Carl Roth, 30% *v/v*) and rinsed in ultrapure water (MQ grade, 18.2 M Ω cm, 1–3 ppb TOC) and hot ultrapure water. The glassy carbon tips (working electrode substrates) were polished on diamond polishing paste (Presi®, 3 and 1 μm). All fresh Ar- and O_2 -saturated electrolytes were prepared from NaOH (Alfa Aesar, 50% *w/w* aqueous solution) and ultrapure water to obtain a concentration of 0.1 M; similarly, NaBH_4 fresh “mother solution” was prepared from previous 0.1 M NaOH solution and NaBH_4 powder (Merck, $\geq 98.0\%$) to obtain a concentration total of 0.5 M.

All electrochemical measurements were performed using a three-electrode PTFE-electrochemical cell with temperature control at 25 °C. The reference electrode was a commercial reversible hydrogen electrode (RHE, Gaskatel GmbH) connected to the cell by a Luggin capillary and the counter electrode was a carbon sheet. The working electrode, a homemade glassy carbon cylinder (glassy carbon Sigradur® from Hochtemperatur-Werkstoffe GmbH) inserted in a PTFE cylinder, was connected to a commercial rotator (Orignalys®). To investigate the electrocatalyst materials, a catalytic layer was made onto the glassy carbon disc substrate (0.196 cm^2) by dropping 20 μL of each prepared ink to obtain a total catalyst loading of 0.8 $\text{mg}_{\text{powder}} \text{cm}^{-2}$. The catalyst inks were prepared by dispersing 10 mg of catalytic powder, 50 μL of 5 wt% Nafion solution (Sigma-Aldrich), 854 μL of isopropanol (Carl Roth), and 372 μL of ultrapure water, followed by ultrasonic homogenization [51]. Then, the electrochemical cell was coupled to an Autolab PGSTAT12 potentiostat to perform RDE (rotating disk electrode) measurements.

An initial reproducible surface state was obtained by applying 50 cyclic voltammograms (CVs) between 0.0 and 1.0 V vs. RHE at 100 mV s^{-1} in Ar-purged 0.1 M NaOH. Next, the CVs of the catalytic layers were recorded in the same conditions at 10 and 5 mV s^{-1} , followed by polarization curves at 5 mV s^{-1} in Ar- and O_2 -saturated 0.1 M NaOH electrolyte at 400 rpm. Capacitive currents obtained (CVs at 5 mV s^{-1}) in Ar-purged electrolyte were subtracted from all polarization curves. This same procedure was repeated after each NaBH_4 addition into the electrolyte (NaBH_4 concentration of 0, 10, 20, 40, and 60 mM). All measurements were corrected from Ohmic drop.

Mass activity ($j_{\text{MA}} = \frac{j_k}{m}$ at 0.85 V vs. RHE, where m is the catalyst mass onto the glassy carbon electrode) was calculated from the kinetic current density for ORR (j_k) obtained by using the Koutecky Levich equation:

$$j_k = -\frac{(j_L j)}{(j_L - j)} \quad (1)$$

where j_L is the O_2 -diffusion limited current density at 0.2 V vs. RHE and j is the Faradaic current corrected as described above.

Results and Discussion

Physicochemical Properties

Detailed physicochemical characterizations of the catalysts have been previously published by Zitolo et al. [48, 53], Choi et al. [50], and Kumar et al. [51]. High-resolution transmission electron microscopy and ^{57}Fe Mössbauer spectroscopy showed that the catalysts with 0.5 wt% metal content before pyrolysis (ca. 1.5 wt% metal content after pyrolysis, due to the mass loss of ca. 66% experienced by the sacrificial metal-organic framework ZIF-8 during pyrolysis) feature only atomically-dispersed metal atoms coordinated by nitrogen atoms and embedded into a carbon matrix (FeN_x sites). In contrast, the catalysts prepared with 5.0 wt% metal content before pyrolysis (ca. 15 wt% metal after pyrolysis) resulted in either metallic (Co) or metal carbide (Fe_3C) nanoparticles surrounded by a carbon–nitrogen shell. No atomically-dispersed metal atoms coordinated by nitrogen atoms were detected from the spectroscopic characterization of these samples. The Mössbauer or EXAFS spectroscopic detection limit for FeN_x sites is ca. 5% relative to the total amount of Fe; so the absence of detection of FeN_x sites monitored by these techniques for the 5.0 wt%-loaded Fe–N–C sample (ca. 15 wt% Fe total content after pyrolysis) means that, at maximum, 0.75 wt% Fe might be present as FeN_x sites in this catalyst. In comparison, the 0.5 wt%-loaded Fe–N–C sample (1.5 wt% Fe bulk content after pyrolysis) only contains FeN_x

sites, and this implies that the absolute number of FeN_x sites in the latter is at least double than that in the 5.0 wt%-loaded Fe–N–C sample. Raman spectroscopy and X-ray diffraction provided evidences that the content of carbon nanocrystallites (i.e., more graphitic carbon phase, with lower amount of surface defects and oxygen functional groups) increases with the increase of metal content. Because ramp pyrolysis results in slow but continuous escape of the volatile products from ZIF-8 and phenanthroline decomposition, ca. twice higher Brunauer–Emmett–Teller (BET) surface area was observed for the ramp-pyrolyzed Fe catalyst with 0.5 wt% Fe content compared with the flash pyrolyzed one [49]. However, this change mostly results in higher microporous surface area but little affects the meso- and macroporous surface areas [49]. In what follows, we refer to the catalysts as M_x mode, where M is Fe or Co, x is the weight percent metal in the powder composed of mixed precursors before pyrolysis, either 0.5 or 5.0 and “mode” is the pyrolysis mode (either ramp or flash pyrolysis, RP and FP, respectively).

Electrochemical Properties

In agreement with our former findings [54], it is found that (i) all the electrocatalyst materials present very interesting ORR activity in alkaline electrolyte and (ii) Fe–N–C electrocatalysts perform better than Co–N–C ones, independently of their structure and BET surface area. To probe their tolerance to sodium borohydride, the electrocatalysts were tested subsequently in NaBH_4 -free and NaBH_4 -containing Ar-saturated electrolytes. Figure 1 shows the cyclic voltammograms obtained at 10 mV s^{-1} for all synthesized catalysts in 0.1 M NaOH electrolytes with different contents of NaBH_4 , in the absence of O_2 . These results reveal that none of the tested electrocatalysts is totally insensitive to the presence of BH_4^- anions in the electrolyte: all of them show non-negligible oxidation current in the “high-potential range,” the magnitude of which increases with the NaBH_4 concentration, signifying that they present some activity towards the electrooxidation of the BH_4^- anion. However, clear differences can be seen when results for Fe–N–C and Co–N–C electrocatalysts are compared.

Focusing firstly on the Fe-containing materials (Fig. 1a), one notices that the 5.0 wt%-loaded Fe–N–C sample is much more sensitive to the presence of NaBH_4 than its 0.5 wt% counterparts (the oxidation current monitored is ca. 10 times larger in the former than in the latter cases). These results are ascribed to the presence of Fe_3C nanoparticles in the $\text{Fe}_{5.0}\text{RP}$ catalyst (which may contain no FeN_x sites at all, and in the most favorable hypothesis for minor fraction of co-existing FeN_x sites, does not contain more FeN_x sites than the $\text{Fe}_{0.5}\text{RP}$ catalyst—see “Physicochemical Properties”), whereas the two other samples ($\text{Fe}_{0.5}\text{FP}$ and $\text{Fe}_{0.5}\text{RP}$) exclusively contain atomically-dispersed iron coordinated by nitrogen ligands (FeN_x sites). It is believed that the lower reactivity of

the $\text{Fe}_{0.5}$ catalysts is related to the absence (or limited amounts) of neighbor sites required for the BH_4^- anion adsorption and its subsequent oxidation. Comparing the Fe–N–C electrocatalysts prepared by the ramp pyrolysis (RP) or the flash pyrolysis (FP), results do not enable to differentiate the samples: $\text{Fe}_{0.5}\text{RP}$ and $\text{Fe}_{0.5}\text{FP}$ present similar reactivity in the presence of NaBH_4 and are leading to very moderate BOR current (both contain atomically-dispersed iron).

Co-containing samples are, at given metal fraction, far more reactive for the BOR than their Fe-containing counterparts. $\text{Co}_{0.5}\text{RP}$, although presenting atomically-dispersed Co coordinated by N-ligands, leads to significant BOR currents particularly for NaBH_4 concentration higher than 20 mM, and the situation is even worse for the $\text{Co}_{5.0}\text{RP}$ sample, which is constituted of Co nanoparticles (Fig. 1b, see inserted image for better visualization). In this last case, the electrode process must involve significant H_2 release by BH_4^- hydrolysis, as evidenced by the instability of the catalyst thin-film, which prevented measurements for NaBH_4 concentrations above 20 mM. These results illustrate the high ability of Co–N–C electrocatalysts to promote reactions with NaBH_4 . This property is not surprising for the $\text{Co}_{5.0}\text{RP}$ sample, owing to the already-reported activity of Co electrocatalysts for the BOR [55, 56] or for the hydrolysis of BH_4^- followed by hydrogen release and subsequent oxidation [57–59]. The present results show that atomically-dispersed Co is also a good BOR electrocatalyst (Hannauer et al. reported the activity of Co^{x+} ($x = 2, 3$) cations for BH_4^- hydrolysis [60], but not for the BOR).

The electrocatalysts were then tested for the ORR in the absence and presence of NaBH_4 at several concentrations in O_2 -saturated electrolytes (Fig. 2). In all cases, the “direct” measurement of the ORR in the presence of NaBH_4 (represented by the curves (3), in symbols) are compared with the “reconstructed” ones, for which the ORR currents in absence of NaBH_4 are added to the currents of BH_4^- oxidation in Ar-saturated supporting electrolyte (represented by the curves (4 + 2), in dotted lines). For the majority of the electrocatalysts considered, the “direct” and “reconstructed” curves of ORR in the presence of NaBH_4 are nearly-superposed; this means that the processes at stake on these class of materials are indeed the sum of the ORR and of the BOR (or of BH_4^- hydrolysis followed by the oxidation of the produced H_2), meaning that the processes are independent from each other.

Furthermore, one clearly sees that not all the electrocatalysts have the same reactivity for the ORR in the presence of NaBH_4 , in agreement to the conclusions obtained from Fig. 1. Firstly, Fe–N–C electrocatalysts presenting only atomically-dispersed iron ($\text{Fe}_{0.5}\text{RP}$ and $\text{Fe}_{0.5}\text{FP}$) are somewhat tolerant to NaBH_4 : the ORR activity in presence of 10 mM NaBH_4 is hardly changed compared with its value in absence of NaBH_4 . However, increasing the NaBH_4 concentration progressively from 10 to 60 mM leads to an increase of BOR contribution to the total current,

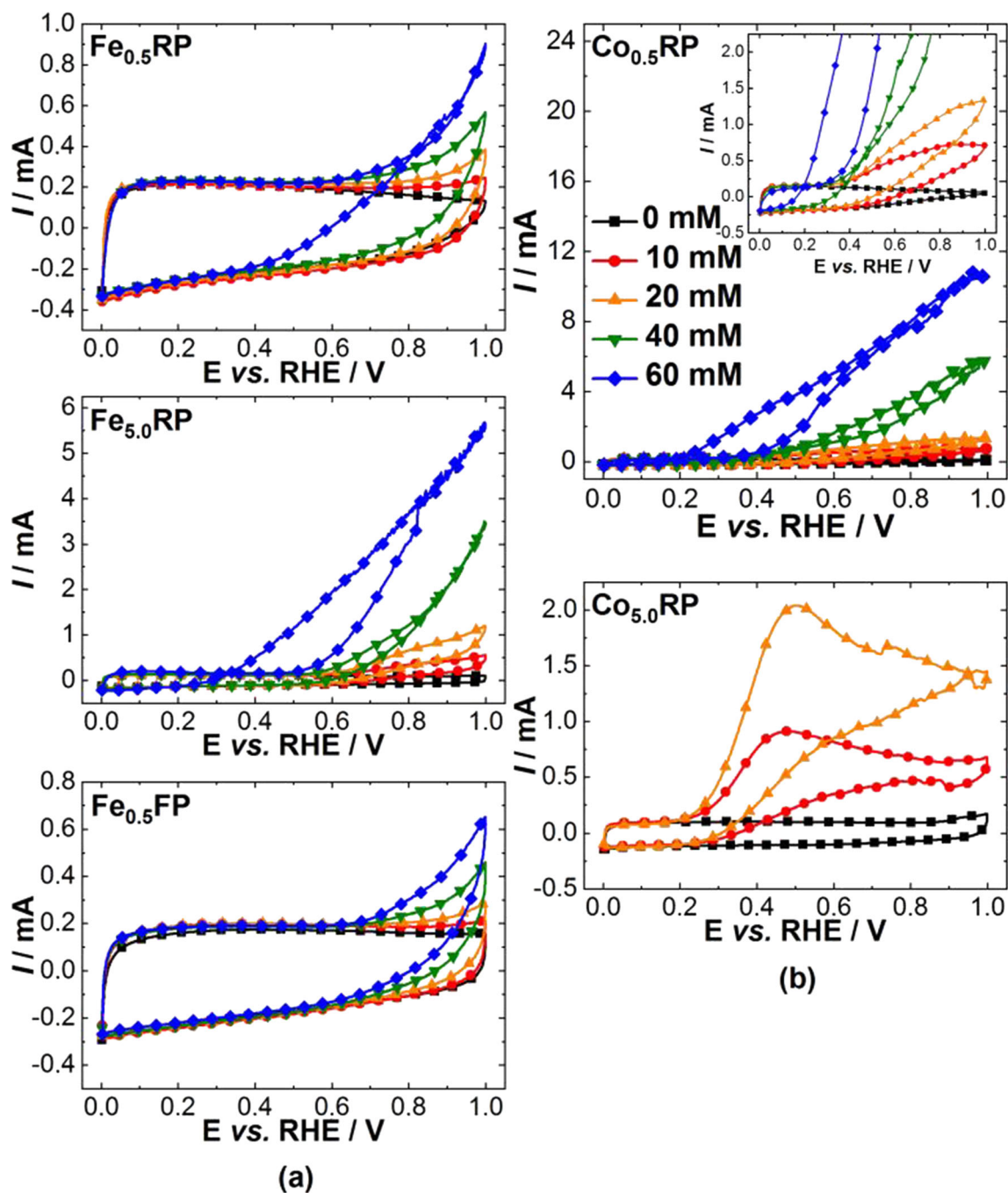


Fig. 1 Cyclic voltamperograms measured on **a** Fe–N–C and **b** Co–N–C electrocatalysts in Ar-purged 0.1 M NaOH supporting electrolyte containing increasing concentrations of NaBH_4 : 0, 10, 20, 40, and 60 mM. All the tests were performed at 25 °C and 10 mV s^{-1} ; the M–N–C

causing a slight negative shift of the apparent ORR onset potential (a sign of depreciated ORR kinetics and/or appearance of mixed electrode potentials, Fig. 2a). Surprisingly, increasing NaBH_4 concentrations lead to practically unaffected absolute value of the ORR-limiting currents (see curves (3), symbols), which one could associate to similar number of electrons involved in ORR electrocatalysis even in the presence of strong reducer. Another interesting aspect is the smaller “direct” ORR-

electrocatalyst loading on the RDE tip was in all measurements $0.8 \text{ mg}_{\text{powder}} \text{ cm}^{-2}$. For the $\text{Co}_{5.0}\text{RP}$ sample, the active layer was destroyed for $[\text{NaBH}_4] > 20 \text{ mM}$

limiting currents compared with the sum of the ORR and the BOR (see curves (4 + 2), dotted lines); it can be related to the reduction of oxygen by BH_4^- anions on the catalysts surface, which in fact reduces the local effective concentration of O_2 in the “direct” measurements.

In contrast, when Fe_3C nanoparticles are present ($\text{Fe}_{5.0}\text{RP}$), the BH_4^- tolerance is no longer maintained: the ORR activity of $\text{Fe}_{5.0}\text{RP}$ is severely affected by increasing amounts of

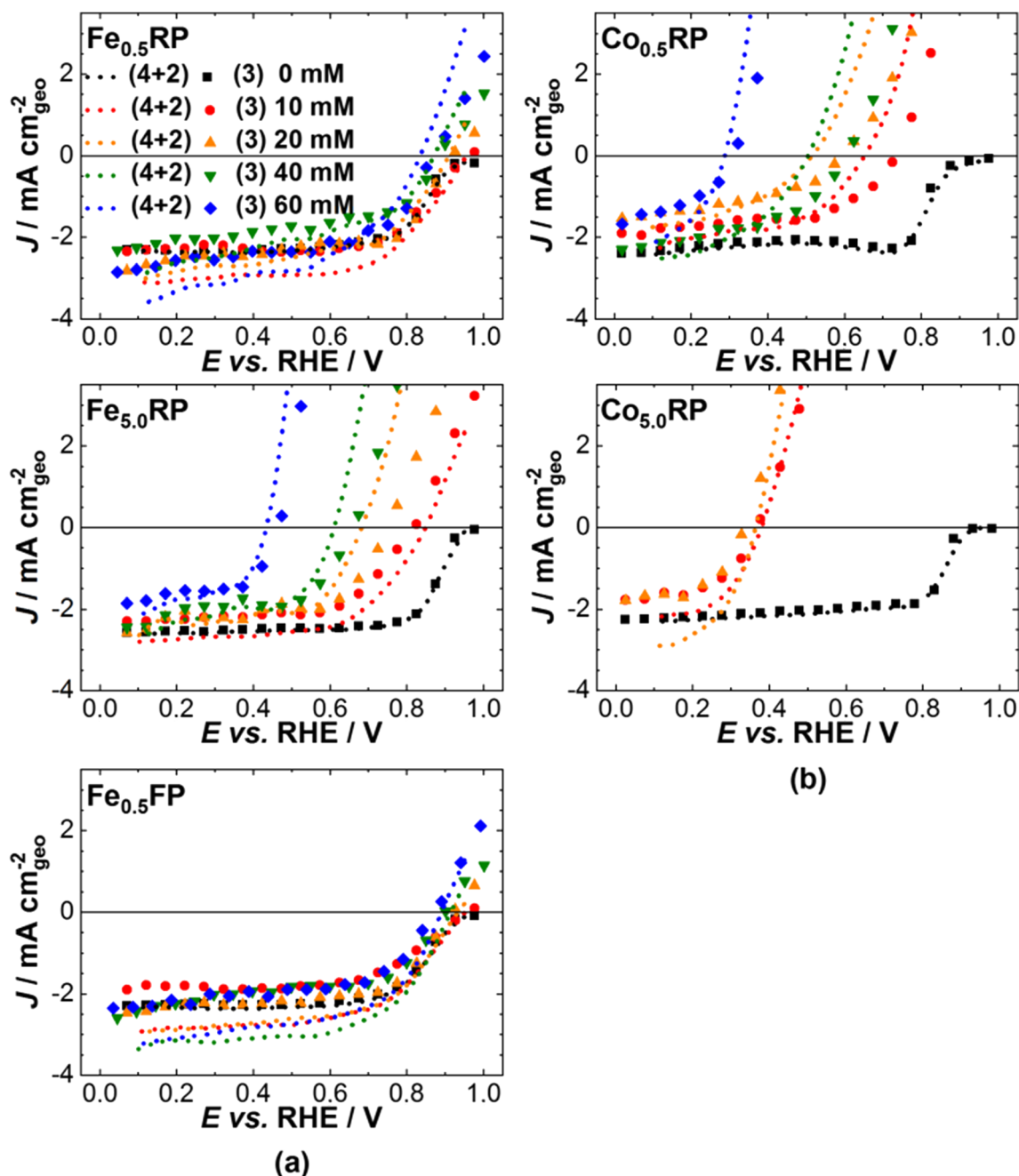


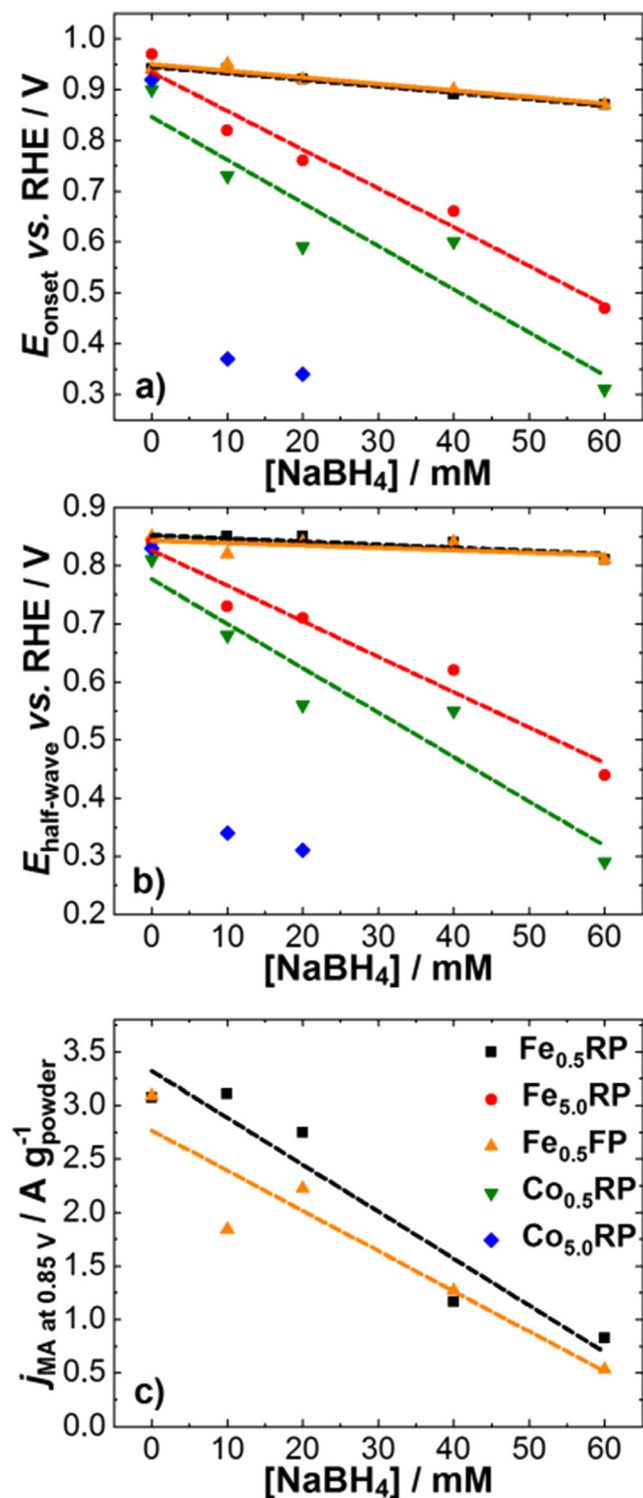
Fig. 2 Cyclic voltamperograms of oxygen reduction reaction measured on **a** Fe–N–C and **b** Co–N–C electrocatalysts in O_2 -purged 0.1 M NaOH supporting electrolyte containing increasing concentrations of $NaBH_4$: 0, 10, 20, 40, and 60 mM. All the tests were performed at 25 °C, 400 rpm,

$NaBH_4$, and even at 10 mM $NaBH_4$, the reaction onset potential is severely negatively shifted (by more than 100 mV; the negative shift being > 400 mV for 60 mM $NaBH_4$). Moreover, increasing $NaBH_4$ concentration leads to decreased absolute values of ORR-limiting currents, which indicates a lower number of electrons involved in the O_2 electrocatalysis and/or a drastic reduction of O_2 concentration in the catalyst surface (probably because of a reaction of O_2 or ORR intermediates (i.e., HO_2^-) with BH_4^- or H_2 [36]). Not surprisingly, Co–

and 5 mV s^{-1} ; the M–N–C electrocatalyst loading on the RDE tip was in all measurements $0.8\text{ mg}_{\text{powder}}\text{ cm}^{-2}$. (symbols) “direct” experimental curves of ORR in the presence of $NaBH_4$; (dotted lines) sum of current of ORR in absence of $NaBH_4$ with those for the BOR (similar as Fig. 1)

N–C samples, which showed non-negligible activity towards the BOR (Fig. 1), are not capable to maintain their good ORR activity in presence of $NaBH_4$ in the electrolyte, even at low concentration (Fig. 2b). Of course, in the presence of Co nanoparticles ($Co_{5.0}RP$), the $NaBH_4$ tolerance is even worse as compared with that of atomically-dispersed Co ($Co_{0.5}RP$).

The ORR onset potential (E_{onset}), half-wave potential ($E_{\text{half-wave}}$), and mass activity (j_{MA} at 0.85 V vs. RHE) of all the electrocatalysts were determined in the “direct” ORR



experiments as a function of the NaBH₄ concentration in the electrolyte, as shown in Fig. 3. The drastic reduction of the onset and half-wave potentials observed in Fig. 3a, b confirms that for Fe_{5.0}RP or Co–N–C samples (Co_{0.5}RP and the Co_{5.0}RP), the tolerance to NaBH₄ is insufficient: these electrocatalysts present highly degraded ORR performances both in the kinetically-controlled and in the mixed kinetic-

Fig. 3 Determination of representative oxygen reduction reaction kinetic parameters for the Fe–N–C and Co–N–C electrocatalysts measured in O₂-purged 0.1 M NaOH supporting electrolyte containing increasing concentrations of NaBH₄: 0, 10, 20, 40, and 60 mM. All the tests were performed at 25 °C, 400 rpm, and 5 mV s⁻¹; the M–N–C electrocatalyst loading on the RDE tip was in all measurements 0.8 mg_{powder} cm⁻². **a** ORR onset potential and **b** ORR half-wave potential, measured for all the M–N–C electrocatalysts; **c** ORR mass activities measured at 0.85 V vs. RHE (corrected from mass-transfer limitation) for the atomically-dispersed Fe–N–C electrocatalysts (the measurement made no sense for the other electrocatalysts)

diffusion-controlled regions as soon as some NaBH₄ is present in the electrolyte.

In this way, the results evidence that only the atomically-dispersed Fe–N–C electrocatalysts present a sufficient tolerance to BH₄⁻ to be used as ORR electrocatalysts in a DBFC cathode, even though their ORR performances would start to non-negligibly decrease if the crossover of NaBH₄ is significant and the BH₄⁻ concentration at the cathode exceeds a few 10 mM. This is further highlighted by results in Fig. 3c, which demonstrate that the intrinsic mass activity of the Fe_{0.5}RP and Fe_{0.5}FP electrocatalysts is not drastically affected by concentrations of NaBH₄ in the NaOH supporting electrolyte, at least for BH₄⁻ concentrations of the order of 10 mM. These results also show that the electrocatalyst prepared by ramp pyrolysis (Fe_{0.5}RP) is a little more tolerant than the one prepared by flash pyrolysis (Fe_{0.5}FP). This behavior may be related to the abovementioned difference in BET surface area, which facilitates the access of oxygen molecules. Note however that this effect progressively vanishes by increasing [BH₄⁻] concentrations in solution to values that far exceed the O₂ solubility (1–2 mM).

Conclusions

The present study shows that by tuning the nature of the metal center, its structure (atomic dispersion vs. nanoparticles) and the BET surface area of the carbonaceous structure, the tolerance of the ORR to NaBH₄, can be enhanced in the potential range of a direct borohydride fuel cell cathode. Evidences of a positive structural effect on the tolerance to BH₄⁻ competition were obtained for catalysts containing atomically-dispersed Fe and Co sites, the latter being magnified for Fe-containing electrocatalysts because of combined poor activity towards the BOR and high activity towards the ORR. A small but non-negligible effect of the microporous surface area was observed; however, it is believed that it relates to higher density of active sites in catalysts after ramp compared with flash pyrolysis. These findings thus open the door to enhanced electrocatalysts for the DBFC both at atomic and macroscopic levels.

Funding Information This study was financially supported by the French National Research Agency through the CAT2CAT (grant number ANR-16-CE05-0007), MobiDiC (grant number ANR-16-CE05-0009) and ANIMA (grant number ANR-19-CE05-0039) projects. R.S. gratefully acknowledges the Coordenação de Aperfeiçoamento de Pessoal de Nível Superior (CAPES), Brazil (grant number: 1614344), CAPES/COFECUB program (grant numbers: 88887-187755/2018-00 and Ph-C 914/18) for funding his research stay at LEPMI and the São Paulo State Research Foundation (FAPESP—grant number: 2013/16930-7) for financial supports. Some material analyses have been performed within “CEMAM,” the Centre of Excellence of Multifunctional Architected Materials (no. ANR-10-LABX-44-01).

References

1. T.B. Reddy, D. Linden, *Linden's Handbook of Batteries*, 4th edn. (McGraw-Hill Professional, New York, 2010)
2. W. Vielstich, A. Lamm, H.A. Gasteiger, *Handbook of Fuel Cells: Fundamentals, Technology and Applications* (Wiley, Chichester, 2003)
3. S. Wasmus, A. Küver, Methanol oxidation and direct methanol fuel cells: a selective review. *J. Electroanal. Chem.* **461**(1-2), 14–31 (1999)
4. W. Vielstich, H.A. Gasteiger, H. Yokokawa, *Handbook of fuel cells: Fundamentals, technology and applications* (Wiley, Chichester, 2009)
5. J.S. Spendlow, A. Wieckowski, Electrocatalysis of oxygen reduction and small alcohol oxidation in alkaline media. *Phys. Chem. Chem. Phys.* **9**(21), 2654–2675 (2007)
6. J.H. Wee, Which type of fuel cell is more competitive for portable application: direct methanol fuel cells or direct borohydride fuel cells? *J. Power Sources* **161**(1), 1–10 (2006)
7. U.B. Demirci, Direct liquid-feed fuel cells: thermodynamic and environmental concerns. *J. Power Sources* **169**(2), 239–246 (2007)
8. S.C. Amendola, P. Onnerud, M.T. Kelly, P.J. Petillo, S.L. Sharp-Goldman, M. Binder, A novel high power density borohydride-air cell. *J. Power Sources* **84**(1), 130–133 (1999)
9. C. Kim, K.-J. Kim, M.Y. Ha, Investigation of the characteristics of a stacked direct borohydride fuel cell for portable applications. *J. Power Sources* **180**(1), 114–121 (2008)
10. B.H. Liu, Z.P. Li, Current status and progress of direct borohydride fuel cell technology development. *J. Power Sources* **187**(2), 291–297 (2009)
11. J. Ma, N.A. Choudhury, Y. Sahai, A comprehensive review of direct borohydride fuel cells. *Renew. Sust. Energ. Rev.* **14**(1), 183–199 (2010)
12. G. Rostamikia, M.J. Janik, Direct borohydride oxidation: mechanism determination and design of alloy catalysts guided by density functional theory. *Energy Environ. Sci.* **3**(9), 1262–1274 (2010)
13. M. Chatenet, M.B. Molina-Concha, J.-P. Diard, First insights into the borohydride oxidation reaction mechanism on gold by electrochemical impedance spectroscopy. *Electrochim. Acta* **54**(6), 1687–1693 (2009)
14. D.A. Finkelstein, N. Da Mota, J.L. Cohen, H.D. Abruña, Rotating disk electrode (RDE) investigation of BH_4^- and BH_3OH^- electro-oxidation at Pt and Au: implications for BH_4^- fuel cells. *J. Phys. Chem. C* **113**(45), 19700–19712 (2009)
15. B. M. Concha, M. Chatenet, E.A. Ticianelli, F.H.B. Lima, In situ infrared (FTIR) study of the mechanism of the borohydride oxidation reaction on smooth Pt electrode. *J. Phys. Chem. C* **115**(25), 12439–12447 (2011)
16. P.-Y. Olu, A. Bonnefont, M. Rouhet, S. Bozdech, N. Job, M. Chatenet, E. Savinova, Insights into the potential dependence of the borohydride electrooxidation reaction mechanism on platinum nanoparticles supported on ordered carbon nanomaterials. *Electrochim. Acta* **179**, 637–646 (2015)
17. M.C.S. Escaño, R.L. Arevalo, E. Gyenge, H. Kasai, Electrocatalysis of borohydride oxidation: a review of density functional theory approach combined with experimental validation. *J. Phys. Condens. Matter* **26**(35), (2014)
18. P.-Y. Olu, A. Bonnefont, M. Chatenet, "Borohydride Oxidation Reaction (BOR) at Pt and Au electrodes: From experimental insights to mechanism and kinetic modeling". In *Encyclopedia Interfacial Chemistry: Surface Science and Electrochemistry*, K. Wandelt (Ed.). (Elsevier, 2018), pp. 384–392
19. P.-Y. Olu, A. Zadick, N. Job, M. Chatenet, "Anode Electrocatalysts for Direct Borohydride and Direct Ammonia Borane Fuel Cells". In *Electrocatalysts for Low Temperature Fuel Cells: Fundamentals and Recent Trends*, T. Maiyalagan, V. S. Saji (Eds.). (Wiley, 2017), pp. 317–346
20. I. Merino-Jiménez, C. Ponce De León, A.A. Shah, F.C. Walsh, Developments in direct borohydride fuel cells and remaining challenges. *J. Power Sources* **219**, 339–357 (2012)
21. K.S. Freitas, B.M. Concha, E.A. Ticianelli, M. Chatenet, Mass transport effects in the borohydride oxidation reaction—influence of the residence time on the reaction onset and faradaic efficiency. *Catal. Today* **170**(1), 110–119 (2011)
22. S. Suda, "Aqueous borohydride solutions". In *Handbook of Fuel Cells - Fundamentals, Technology and Applications*, W. Vielstich, A. Lamm, H. A. Gasteiger (Eds.). (Wiley, Chichester, 2003), pp. 115–120
23. C. Ponce De León, F. C. Walsh, "Direct and indirect borohydride fuel cells". In *Reference Module in Chemistry: Molecular Sciences and Chemical Engineering* (Elsevier, 2015). <https://doi.org/10.1016/B978-0-12-409547-2.11190-4>
24. Z. Wang, J. Parrondo, C. He, S. Sankarasubramanian, V. Ramani, Efficient pH-gradient-enabled microscale bipolar interfaces in direct borohydride fuel cells. *Nat. Energy* **4**, 281–289 (2019)
25. M. Chatenet, Tailoring membranes. *Nat. Energy* **4**, 261–262 (2019)
26. S. Ould-Amara, J. Dillet, S. Didierjean, M. Chatenet, G. Maranzana, Operating heterogeneities within a direct borohydride fuel cell. *J. Power Sources* **439**, 227099 (2019)
27. K. N. Mochalov, V. S. Khain, G. G. Gil'manshin, A generalized scheme for the hydrolysis of the borohydride ion and diborane. *Dokl. Akad. Nauk SSSR* **162**(3), 613–616 (1965)
28. M.M. Kreevoy, R.W. Jacobson, The rate of decomposition of NaBH_4 in basic aqueous solutions. *Vent. Alembic* **15**, 2–3 (1979)
29. D. Sebastián, A. Serov, I. Matanovic, K. Artyushkova, P. Atanassov, A.S. Aricò, V. Baglio, Insights on the extraordinary tolerance to alcohols of Fe-N-C cathode catalysts in highly performing direct alcohol fuel cells. *Nano Energy* **34**, 195–204 (2017)
30. K.B. Ma, D.H. Kwak, S.B. Han, H.S. Park, D.H. Kim, J.E. Won, S.H. Kwon, M.C. Kim, S.H. Moon, K.W. Park, Direct ethanol fuel cells with superior ethanol-tolerant nonprecious metal cathode catalysts for oxygen reduction reaction. *ACS Sustain. Chem. Eng.* **6**(6), 7609–7618 (2018)
31. L. Osmieri, R. Escudero-Cid, A.H.A. Monteverde Videla, P. Ocón, S. Specchia, Application of a non-noble Fe-N-C catalyst for oxygen reduction reaction in an alkaline direct ethanol fuel cell. *Renew. Energy* **115**, 226–237 (2018)
32. A.C. Garcia, J.J. Linares, M. Chatenet, E.A. Ticianelli, NiMnO_x/C: a non-noble ethanol-tolerant catalyst for oxygen reduction in alkaline exchange membrane DEFC. *Electrocatalysis* **5**, 41–49 (2014)
33. E. A. Ticianelli, F. H. B. Lima, "Nanostructured Electrocatalysts for Methanol and Ethanol-Tolerant Cathodes". In *Direct Alcohol Fuel Cells: Materials, Performance, Durability and Applications*, H. R. Corti, E. R. Gonzalez (Eds.). (Springer, 2014), pp. 99–119

34. X. Yang, S. Li, Y. Liu, X. Wei, Y. Liu, $\text{LaNi}_{0.8}\text{Co}_{0.2}\text{O}_3$ as a cathode catalyst for a direct borohydride fuel cell. *J. Power Sources* **196**(11), 4992–4995 (2011)
35. M. Chatenet, F. Micoud, I. Roche, E. Chainet, J. Vondrák, Kinetics of sodium borohydride direct oxidation and oxygen reduction in sodium hydroxide electrolyte: Part II. O_2 reduction. *Electrochim. Acta* **51**(25), 5452–5458 (2006)
36. A.C. Garcia, F.H.B. Lima, E.A. Ticianelli, M. Chatenet, Carbon-supported nickel-doped manganese oxides as electrocatalysts for the oxygen reduction reaction in the presence of sodium borohydride. *J. Power Sources* **222**, 305–312 (2013)
37. I. Roche, E. Chainet, M. Chatenet, J. Vondrák, Durability of carbon-supported manganese oxide nanoparticles for the oxygen reduction reaction (ORR) in alkaline medium. *J. Appl. Electrochem.* **38**, 1195–1201 (2008)
38. H. Cheng, K. Scott, Investigation of non-platinum cathode catalysts for direct borohydride fuel cells. *J. Electroanal. Chem.* **596**(2), 117–123 (2006)
39. M. Chatenet, F. Micoud, I. Roche, E. Chainet, Kinetics of sodium borohydride direct oxidation and oxygen reduction in sodium hydroxide electrolyte: Part I. BH_4^- electro-oxidation on Au and Ag catalysts. *Electrochim. Acta* **51**(25), 5459–5467 (2006)
40. M.H. Atwan, D.O. Northwood, E.L. Gyenge, Evaluation of colloidal Ag and Ag-alloys as anode electrocatalysts for direct borohydride fuel cells. *Int. J. Hydrog. Energy* **32**(15), 3116–3125 (2007)
41. A.V. N. Kumar, S. Harish, J. Joseph, New route for synthesis of electrocatalytic $\text{Ni}(\text{OH})_2$ modified electrodes—electrooxidation of borohydride as probe reaction. *Bull. Mater. Sci.* **37**, 635–641 (2014)
42. D.M.F. Santos, B. Šljukić, L. Amaral, D. Macciò, A. Saccone, C.A.C. Sequeira, Nickel and nickel-cerium alloy anodes for direct borohydride fuel cells. *J. Electrochem. Soc.* **161**(5), F594–F599 (2014)
43. A.G. Oshchepkov, G. Braesch, S. Ould-Amara, G. Rostamikia, G. Maranzana, A. Bonnefont, V. Papaefthimiou, M.J. Janik, M. Chatenet, E.R. Savinova, Nickel metal nanoparticles as anode electrocatalysts for highly efficient direct borohydride fuel cells. *ACS Catal.* **9**(9), 8520–8528 (2019)
44. A. Serov, A. Aziznia, P.H. Benhangi, K. Artyushkova, P. Atanassov, E. Gyenge, Borohydride-tolerant oxygen electroreduction catalyst for mixed-reactant Swiss-roll direct borohydride fuel cells. *J. Mater. Chem. A* **1**(45), 14384–14391 (2013)
45. M. Lefèvre, E. Proietti, F. Jaouen, and J.-P. Dodelet, Iron-based catalysts with improved oxygen reduction activity in polymer electrolyte fuel cells. *Science* **324** (5923), 71–74 (2009)
46. A. Serov, K. Artyushkova, E. Niangar, C. Wang, N. Dale, F. Jaouen, M.T. Sougrati, Q. Jia, S. Mukerjee, P. Atanassov, Nanostructured non-platinum catalysts for automotive fuel cell application. *Nano Energy* **16**, 293–300 (2015)
47. F. Luo, C.H. Choi, M.J.M. Primbs, W. Ju, S. Li, N.D. Leonard, A. Thomas, F. Jaouen, P. Strasser, Accurate evaluation of active-site density (SD) and turnover frequency (TOF) of PGM-free metal-nitrogen-doped carbon (MNC) electrocatalysts using CO cryo adsorption. *ACS Catal.* **9**(6), 4841–4852 (2019)
48. A. Zitolo, N. Ranjbar-Sahraie, T. Mineva, J. Li, Q. Jia, S. Stamatina, G. F. Harrington, S. M. Lyth, P. Krtil, S. Mukerjee, E. Fonda, F. Jaouen, Identification of catalytic sites in cobalt-nitrogen-carbon materials for the oxygen reduction reaction. *Nat. Comm.* **8**, 957 (2017).
49. V. Armel, J. Hannauer, F. Jaouen, Effect of ZIF-8 crystal size on the O_2 electro-reduction performance of pyrolyzed Fe–N–C catalysts. *Catalysts* **5**(3), 1333–1351 (2015)
50. C.H. Choi, H.K. Lim, M.W. Chung, G. Chon, N. Ranjbar Sahraie, A. Altin, M.T. Sougrati, L. Stievano, H.S. Oh, E.S. Park, F. Luo, P. Strasser, G. Dražić, K.J.J. Mayrhofer, H. Kim, F. Jaouen, The Achilles’ heel of iron-based catalysts during oxygen reduction in an acidic medium. *Energy Environ. Sci.* **11**, 3176–3182 (2018)
51. K. Kumar, P. Gairola, M. Lions, N. Ranjbar-Sahraie, M. Mermoux, L. Dubau, A. Zitolo, F. Jaouen, F. Maillard, Physical and chemical considerations for improving catalytic activity and stability of non-precious-metal oxygen reduction reaction catalysts. *ACS Catal.* **8**(12), 11264–11276 (2018)
52. V. Goellner, V. Armel, A. Zitolo, E. Fonda, F. Jaouen, Degradation by hydrogen peroxide of metal-nitrogen-carbon catalysts for oxygen reduction. *J. Electrochem. Soc.* **162**(6), H403–H414 (2015)
53. A. Zitolo, V. Goellner, V. Armel, M.T. Sougrati, T. Mineva, L. Stievano, E. Fonda, F. Jaouen, Identification of catalytic sites for oxygen reduction in iron- and nitrogen-doped graphene materials. *Nat. Mater.* **14**(9), 937–942 (2015)
54. R. Sgarbi, K. Kumar, F. Jaouen, A. Zitolo, E. A. Ticianelli, and F. Maillard, Oxygen reduction reaction mechanism and kinetics on $\text{M-N}_x\text{C}_y$ and M@N-C active sites present in model M–N–C catalysts under alkaline and acidic conditions. *J. Solid State Electrochem.* (2019). <https://doi.org/10.1007/s10008-019-04436-w>
55. J. Ma, X. Gao, D. Wang, T. Xue, S. Yang, Effect of cobalt precursors on Co_3O_4 anodic catalyst for a membrane-free direct borohydride fuel cell. *J. Alloys Compd.* **724**, 474–480 (2017)
56. A. Tiwari, V. Singh, T.C. Nagaiah, Non-noble cobalt tungstate catalyst for effective electrocatalytic oxidation of borohydride. *ACS Appl. Mater. Interfaces* **11**(24), 21465–21472 (2019)
57. A. Garron, D. Świerczyński, S. Bennici, A. Auroux, New insights into the mechanism of H_2 generation through NaBH_4 hydrolysis on Co-based nanocatalysts studied by differential reaction calorimetry. *Int. J. Hydrog. Energy* **34**(3), 1185–1199 (2009)
58. J. Choi, J. Chung, Preparation and Characteristics of Novel Cobalt Oxide Catalysts for Hydrogen Generation from Metal Borohydride Solution. *J. Energy Eng.* **142**(3), (2016)
59. R. Edla, S. Gupta, N. Patel, N. Bazzanella, R. Fernandes, D.C. Kothari, A. Miotello, Enhanced H_2 production from hydrolysis of sodium borohydride using Co_3O_4 nanoparticles assembled coatings prepared by pulsed laser deposition. *Appl. Catal. A Gen.* **515**, 1–9 (2016)
60. J. Hannauer, U.B. Demirci, C. Geantet, J.M. Herrmann, P. Miele, Enhanced hydrogen release by catalyzed hydrolysis of sodium borohydride-ammonia borane mixtures: a solution-state ^{11}B NMR study. *Phys. Chem. Chem. Phys.* **13**(9), 3809–3818 (2011)